

Rescue of Volume-regulated Anion Current by Bestrophin Mutants with Altered Charge Selectivity

Li-Ting Chien and H. Criss Hartzell

Department of Cell Biology and Center for Neurodegenerative Disease, Emory University School of Medicine, Atlanta, GA 30322

Mutations in human bestrophin-1 are linked to various kinds of retinal degeneration. Although it has been proposed that bestrophins are Ca^{2+} -activated Cl^- channels, definitive proof is lacking partly because mice with the bestrophin-1 gene deleted have normal Ca^{2+} -activated Cl^- currents. Here, we provide compelling evidence to support the idea that bestrophin-1 is the pore-forming subunit of a cell volume-regulated anion channel (VRAC) in *Drosophila* S2 cells. VRAC was abolished by treatment with RNAi to *Drosophila* bestrophin-1. VRAC was rescued by overexpressing bestrophin-1 mutants with altered biophysical properties and responsiveness to sulfhydryl reagents. In particular, the ionic selectivity of the F81C mutant changed from anionic to cationic when the channel was treated with the sulfhydryl reagent, sodium (2-sulfonatoethyl) methanethiosulfonate (MTSES^-) ($P_{\text{Cs}}/P_{\text{Cl}} = 0.25$ for native and 2.38 for F81C). The F81E mutant was 1.3 times more permeable to Cs^+ than Cl^- . The finding that VRAC was rescued by F81C and F81E mutants with different biophysical properties shows that bestrophin-1 is a VRAC in S2 cells and not simply a regulator or an auxiliary subunit. F81C overexpressed in HEK293 cells also exhibits a shift of ionic selectivity after MTSES^- treatment, although the effect is quantitatively smaller than in S2 cells. To test whether bestrophins are VRACs in mammalian cells, we compared VRACs in peritoneal macrophages from wild-type mice and mice with both bestrophin-1 and bestrophin-2 disrupted ($\text{best1}^{-/-}/\text{best2}^{-/-}$). VRACs were identical in wild-type and $\text{best1}^{-/-}/\text{best2}^{-/-}$ mice, showing that bestrophins are unlikely to be the classical VRAC in mammalian cells.

INTRODUCTION

Mutations in bestrophin-1 are responsible for several retinopathies, including Best vitelliform macular dystrophy (Marquardt et al., 1998; Petrukhin et al., 1998), adult-onset macular dystrophy (Seddon et al., 2001), autosomal-dominant vitreochoidopathy (Yardley et al., 2004), autosomal-recessive bestrophinopathy (Burgess et al., 2008), and canine multifocal retinopathy (Guziewicz et al., 2007). There is considerable evidence that bestrophins are Cl^- channels (for review see Hartzell et al., 2008). Expression of a variety of different bestrophins in HEK293 cells induces novel Cl^- currents (Sun et al., 2002; Qu et al., 2003, 2004, 2006a, 2006b; Tsunenari et al., 2003, 2006; Qu and Hartzell, 2004; Barro Soria et al., 2006; Chien et al., 2006). Furthermore, mutation of certain amino acids alters the permeability and conductance of the channel (Qu et al., 2004, 2006b; Qu and Hartzell, 2004), and sulfhydryl reagents alter the properties of cysteine-substituted channels in characteristic ways (Tsunenari et al., 2003; Qu and Hartzell, 2004; Qu et al., 2006b). However, the idea that bestrophin-1 is a Cl^- channel has been seriously questioned (Marmorstein

et al., 2004a, 2004b, 2006; Rosenthal et al., 2005; Marmorstein and Kinnick, 2007). This challenge is based largely on several observations, the most compelling of which is that Cl^- currents in retinal pigment epithelial cells are not abolished in mouse bestrophin-1 (mBest1) knockout mice (Marmorstein et al., 2006). Furthermore, it is not clear that the Cl^- channel function of bestrophin can explain the human disease phenotypes (Hartzell et al., 2008). These questions, coupled with the observation that human bestrophin-1 (hBest1) can regulate voltage-gated Ca^{2+} channels (Rosenthal et al., 2005; Yu et al., 2008), has led to the suggestion that hBest1 is not a Cl^- channel but is rather a channel regulator (Marmorstein et al., 2006; Hartzell et al., 2008).

We have previously concluded that *Drosophila* bestrophin-1 (dBest1) is a Cl^- channel that is dually regulated by Ca^{2+} and cell volume and mediates regulatory volume decrease (RVD) in *Drosophila* S2 cells (Chien and Hartzell, 2007). We showed that five different dBest1 RNAi constructs abolished endogenous Cl^- currents activated by intracellular Ca^{2+} or by cell swelling. The loss of these currents could be rescued by overexpression of wild-type dBest1. However, the rescue experiment alone does not formally prove that dBest1 is the pore-forming

Correspondence to H. Criss Hartzell: criss.hartzell@emory.edu

Abbreviations used in this paper: dBest1, *Drosophila* bestrophin-1; DTT, dithiothreitol; GHK, Goldman-Hodgkin-Katz; hBest1, human bestrophin-1; mBest1, mouse bestrophin-1; MTS, methanethiosulfonate; MTSES^- , sodium (2-sulfonatoethyl) MTS; MTSET, 2-trimethylammonioethylmethanethiosulfonate, bromide salt; RVD, regulatory volume decrease; UTR, untranslated region; VRAC, volume-regulated anion channel.

© 2008 Chien and Hartzell. This article is distributed under the terms of an Attribution-Noncommercial-Share Alike-No Mirror Sites license for the first six months after the publication date (see <http://www.jgp.org/misc/terms.shtml>). After six months it is available under a Creative Commons License (Attribution-Noncommercial-Share Alike 3.0 Unported license, as described at <http://creativecommons.org/licenses/by-nc-sa/3.0/>).

subunit of the S2 volume-regulated anion channel (VRAC) because overexpression of an essential regulator or accessory subunit of the channel could have the same effect. Here, we address this issue directly by rescuing VRAC in dBest1 RNAi-treated S2 cells with dBest1 mutants that have altered biophysical properties. Residue F81 (F80 in vertebrates; *Drosophila* has an extra amino acid at position 14) was chosen for this purpose because F81 is invariant among all bestrophins and has been implicated as an important residue in ionic selectivity (Qu et al., 2006b).

Here, we have rescued the VRAC current in S2 cells abolished by dBest1 RNAi by expressing dBest1-F81C. The rescued current is cell volume sensitive but differs from the wild-type current in the shape of the I-V curve, the responsiveness to methanethiosulfonate (MTS) reagents, and anion-cation selectivity. This finding provides strong evidence that dBest1 is indeed the channel pore and is the volume-sensitive Cl⁻ channel in S2 cells. However, VRACs are normal in peritoneal macrophages from mice with both bestrophin-1 and bestrophin-2 disrupted, suggesting that bestrophins are not the classical mammalian VRAC.

MATERIALS AND METHODS

Rescue in S2 Cells and Heterologous Expression

Drosophila S2 cells were cultured in Schneider's *Drosophila* medium (Invitrogen) supplemented with 10% heat-inactivated FBS (Invitrogen) and 50 U/ml penicillin and 50 µg/ml streptomycin (Invitrogen) at room temperature. The open reading frame of dBest1 was introduced into pAc5.1/V5-HisA *Drosophila* expression vector (Invitrogen) as described previously (Chien et al., 2006; Chien and Hartzell, 2007). Residue F81 was mutated to cysteine by a PCR-based site-directed mutagenesis method (Quickchange; Stratagene). The F81C mutation was introduced by PCR primers (up: 5'-CATACCCCTGTCCTGCGTGCTTGGTTTC-3'; down: 5'-GAA-ACCAAGCACGCAGGACAGGGGTATG-3'). pAc5.1-dBest1ORF (open reading frame) was used as the template for high fidelity PCR amplification with Pfu DNA polymerase. The methylated template was digested with the endonuclease Dpn-I, and the non-methylated PCR product was transformed into XL-1 blue *Escherichia coli* for amplification. DNA was sequenced to confirm the mutation. For the rescue experiment, 2×10^5 S2 cells were treated with 8.3 µg of double-stranded RNA against the 5' untranslated region (UTR) of dBest1 (5UdB1) for 4 d (Chien and Hartzell, 2007). The RNAi-treated cells were then transfected with a mixture of pAc5.1-dBest1 or dBest1-F81C cDNA and pAc5.1-EGFP in a 2:1 ratio using calcium phosphate. Green cells were recorded 2–4 d after transfection. Possible off-target effects of 5UdB1 RNAi have been described in detail previously (Chien and Hartzell, 2007). HEK-293 cells were used for heterologous expression of wild-type dBest1 and F81C. HEK-293 cells (American Type Culture Collection) were cultured in Eagle's minimum essential medium with L-glutamine (CellGro), 10% heat-inactivated FBS (Invitrogen), and 50 U/ml penicillin and 50 µg/ml streptomycin (Invitrogen) in 5% CO₂/95% O₂ at 37°C. Transfection was performed as described by Qu et al. (2004). In brief, pcDNA3.1-dBest1 or dBest1-F81C cDNA and pEGFP (Invitrogen) were co-transfected in HEK cells in a 4:1 ratio using Fugene-6 reagent (Roche). Green cells were recorded during the third to fourth day after transfection.

Solutions

The standard extracellular solution (E300) used for patch clamping S2 cells contained 115 mM NaCl, 2 mM CaCl₂, 1 mM MgCl₂, 5 mM KCl, 10 mM HEPES (pH 7.2 with NaOH), and 48 mannitol to achieve 300 mosmol kg⁻¹. The intracellular solution (I300) contained 110 mM CsCl, 10 mM EGTA, 8 mM MgCl₂, 10 mM HEPES, pH 7.2, and 45 mannitol to achieve 300 mosmol kg⁻¹. I340 internal solution was prepared by adding 40 mM mannitol to the I300 solution to achieve 340 mosmol kg⁻¹. Osmotic pressure differences are expressed as Δ mosmol kg⁻¹ (intracellular osmolality minus extracellular osmolality). Unless indicated otherwise, the osmotically sensitive Cl⁻ current was routinely activated by Δ40 mosmol kg⁻¹ osmotic pressure (E300/I340). These combinations of solutions set the E_{rev} for Cl⁻ currents to 0 mV, whereas cation currents carried by Cs⁺ or Na⁺ would have very negative or positive E_{rev}, respectively. The major cation in the intracellular solution was Cs⁺, whereas the standard extracellular cation was Na⁺ unless specified otherwise. Stock solutions of 100 mM 2-trimethylammonioethylmethanethiosulfonate, bromide salt (MTSET⁺) and sodium (2-sulfonatoethyl) methanesulfonate (MTSES⁻) (Toronto Research Chemicals) were prepared in water and stored at -80°C. Aliquots of the MTS stock solution were thawed and kept on ice for no longer than 10 min. 1 mM of working solution was prepared by diluting the stock with the external recording solution immediately before use. Working solutions of dithiothreitol (DTT; Sigma-Aldrich) were prepared freshly from frozen 1-M stock solutions. To determine relative cation⁺/Cl⁻ permeabilities, we used a high Ca²⁺ intracellular solution containing 150 mM CsCl (or NaCl), 10 mM HEPES (pH 7.2 with NMDG), and 5 mM Ca-EGTA-NMDG, and extracellular solutions containing different CsCl (or NaCl) (150, 100, 50, 20, or 10 mM), 10 mM HEPES, and 1 mM CaCl₂. All solutions were pH 7.2 and adjusted to 304 mosmol kg⁻¹ with mannitol.

Electrophysiology, Cell Volume Determination, and Data Analysis

S2 cells were allowed to adhere to the bottom of the recording chamber for ~10 min and were then washed and incubated with extracellular solution for ~10 min before whole cell recording. Fire-polished pipettes pulled from borosilicate glass (Sutter Instrument Co.) had resistances of 2–3 MΩ when filled with intracellular solution. For whole cell recording, cells were voltage clamped with ~1-s duration ramps from -100 to +100 mV run at 10-s intervals (Chien and Hartzell, 2007). Whole cell recording data were filtered at 2–5 kHz and sampled at 5–10 kHz by an Axopatch 200A amplifier controlled by Clampex 8.2 via a Digidata 1322A data acquisition system (MDS Analytical Technologies). Data were not corrected for liquid junction potentials, which were calculated to be <0.6 mV when quantifying relative Cs/Cl permeability. For NaCl solutions, the liquid junction potential was calculated and corrected using Liquid Junction Potential utility in pClamp (the maximum liquid junction potential for 150 mM NaCl inside and 10 mM NaCl outside was -12.6 mV). Series resistance compensation was not routinely used. Relative X/Cl permeability was determined by measuring the shift of E_{rev} upon changing the solution on the extracellular side of the membrane from the one containing 150 mM XCl to 100, 50, 20, and 10 mM. The relative X/Cl permeability ratio was then estimated by fitting the measured mean E_{rev} differences with the Goldman-Hodgkin-Katz (GHK) equation (Hille, 2001), assuming that the movement of anions is independent of cations,

$$P_X/P_{Cl} = \exp(\Delta E_{rev} F/RT),$$

where ΔE_{rev} is the difference between the reversal potential with the test XCl concentration and that observed with symmetrical [XCl] (E_{rev} = 0 mV), and F, R, and T have their normal thermodynamic

meanings. All data were analyzed using pClamp 8.2 software and Origin 7.0 and are expressed as mean \pm SEM. Two sample *t* tests (independent tests) were performed with significance levels of 0.05 or 0.01 for statistical analysis.

Phase contrast images of the cells were taken with a Photometrics Cool-Snap camera and analyzed with MetaMorph Imaging software (MDS Analytical Technologies). The volume of the cell was calculated from the measured circumference assuming that the shape of S2 cells is spherical. Some duplicate measurements were performed blind. With an osmotic pressure difference of 40 mosmol kg⁻¹, one would expect a 13% increase in cell volume if the cell were a perfect osmometer. However, we observed a larger change in cell volume than expected. This might be explained by the fact that cell swelling is not spherically symmetrical, as assumed. If cell swelling is constrained in the *z*-plane by mechanical pressure from the patch pipet, the change in cell volume may appear to be larger than it actually is. For this reason, the estimates of cell volume may be subject to some quantitative error. One would also expect that the cell volume would remain unchanged in isosmotic condition. However, we observed an \sim 13% reduction instead. This could possibly be caused by dilution of cytoplasmic osmolytes into the recording pipet.

Measurement of VRAC in Peritoneal Macrophages

Peritoneal macrophages were isolated by peritoneal lavage. 5 ml of cold RPMI medium containing 10% FBS was injected intraperitoneally into a mouse that had just been killed by an overdose of isoflurane anesthesia. The abdomen was massaged for several minutes, and the fluid was withdrawn and plated onto glass coverslips and cultured at 37°C in a 5% CO₂, 95% air environment. Round macrophages were patch clamped 2 h to 2 d after isolation at room temperature. The intracellular solution was 95 mM Cs-aspartate, 40 mM CsCl, 1 mM MgCl₂, 10 mM HEPES pH 7.4, 4 mM Na/K-ATP, and 5 mM EGTA, and CaCl₂ was added to give \sim 50 nM free Ca²⁺. The hyposmotic extracellular solution was 105 mM NaCl, 6 mM CsCl, 1 mM MgCl₂, 1.5 mM CaCl₂, 10 mM HEPES, pH 7.4, and 10 mM glucose (234 mosmol kg⁻¹). Isosmotic and hyperosmotic solutions were made by adding mannitol to the hyposmotic solution to make 266-, 306-, and 326-mosmol kg⁻¹ solutions. Recording pipets had 3–6 MΩ of resistances when filled with intracellular solution, and the averaged cell capacitance was 12.73 \pm 0.89 pF (*n* = 20). Wild-type mice were C57B. The mBest1-mBest2 double knockout mice were made by breeding mBest1 knockout mice (Merck & Co.) with mBest2 knockout mice (Bakall et al., 2008). The mBest1 knockout mice were generated by homologous recombination that resulted in deletion of exons 5–9 of mBest1.

RESULTS

Rescue of Volume-regulated Chloride Currents in S2 Cells by dBest1-F81C

To test if dBest1 is the VRAC in *Drosophila* S2 cells and not simply a regulator of an endogenous VRAC, we examined whether VRAC could be rescued by expressing a mutant dBest1 that had altered biophysical properties. To do this, endogenous dBest1 was first knocked down by double-stranded interfering RNA to a portion of the 5' UTR of dBest1, as described previously (Chien and Hartzell, 2007). To verify that the dBest1 RNAi was effective in knocking down the current, RNAi-treated cells were patch clamped in each experiment (Fig. 1 B). Then, dBest1 (wild-type, F81C, F81E, or F81L) was ex-

pressed by transient transfection. Both the native and rescued VRAC current was <300 pA under isosmotic conditions (Fig. 1 A) but was activated when the extracellular solution was 40 mosmol kg⁻¹ hyposmotic relative to the internal solution (I340/E300) (Fig. 1 B). As expected, the dBest1-F81C current had different properties than the native VRAC current. The native VRAC current had an outwardly rectifying, S-shaped I-V curve, whereas the F81C current was inwardly rectifying (Figs. 1 B and 3 D). This inwardly rectifying I-V of F81C was similar to the Ca²⁺-activated dBest1-F81C current expressed heterologously in HEK cells (Chien et al., 2006). Transfection with the F81L mutant produced no current (67.0 \pm 26.3 pA; *n* = 5). In contrast, F81C currents increased with time coordinately with cell swelling over several minutes. Immediately after patch break, the F81C currents were 0.4 \pm 0.1 nA at +100 mV. The currents then activated slowly to a mean plateau amplitude of 1.0 \pm 0.3 nA (*n* = 7) with an average half-time of \sim 1.5 min (Fig. 1 C). The activation of the F81C current was coupled to cell swelling. On average, F81C cells swelled 33.6 \pm 0.7% (*n* = 7) when their currents were fully activated with Δ 40 mosmol kg⁻¹ osmotic pressure (Fig. 1 D). F81C currents were volume sensitive because the current failed to activate under isosmotic conditions (Δ 0 mosmol kg⁻¹, E300/I300) and remained <0.3 nA (*n* = 6) throughout \sim 5 min of recording. Cell swelling was not observed with these cells in isosmotic solutions. Instead, their volume decreased 13.8 \pm 2.7% by the end of the recording.

Opposite Effects of MTSET⁺ on dBest1-F81C and Native dBest1

Additional evidence that dBest1 forms the VRAC pore was provided by the finding that MTSET⁺ had opposite effects on the native VRAC current and the rescued dBest1-F81C current. I-V curves and the time course of current development are shown in Fig. 2. MTSET⁺ caused a mean \sim 35% reduction in the amplitude of the native dBest1 VRAC currents (Fig. 3, A and B) over 8–10 min. The effect of MTSET⁺ on native cells was not reversible by 5 mM DTT. In contrast, MTSET⁺ caused a dramatic augmentation in the F81C current. On average, the current was transiently increased 15-fold, followed by a gradual decline to a level that was still elevated approximately four- to sevenfold compared with the F81C currents before MTSET⁺ (Fig. 3, A and B). The stimulation by MTSET⁺ was at least partly reversible by DTT. In addition to stimulating the current, MTSET⁺ converted the F81C current from slightly inwardly rectifying to slightly outwardly rectifying and shifted *E*_{rev} 1.9 \pm 0.7 mV in the positive direction (Fig. 3 C). Although this shift was small, it was in the opposite direction to the shift produced by MTSES⁻ (see below).

MTSES⁻ Increases the Cation Permeability of dBest1-F81C
The effect of MTSES⁻ on the I-V relationships of native and F81C-rescued cells is shown in Fig. 4 (A and B).

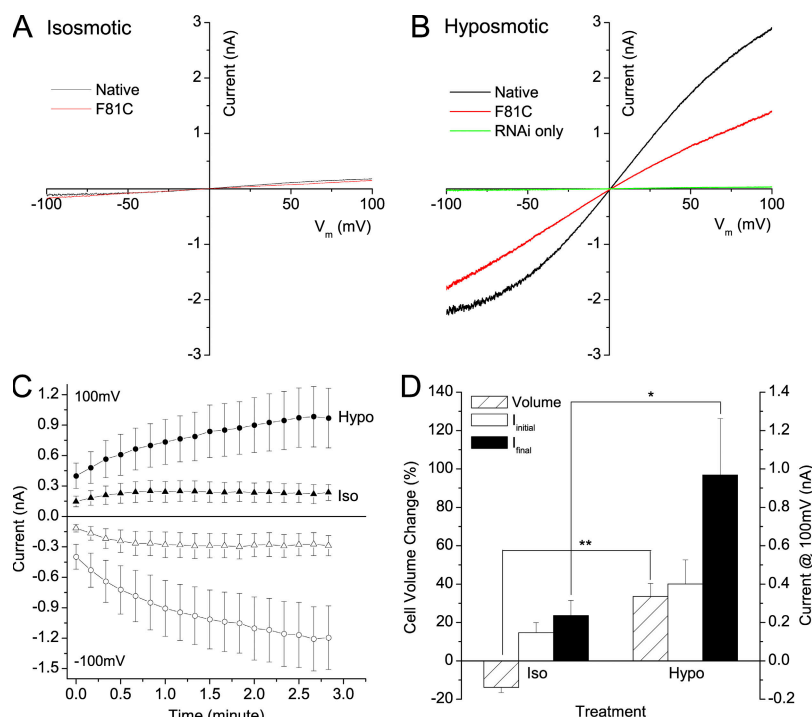


Figure 1. Rescue of the volume-regulated Cl^- current in S2 cells by expression of dBest1-F81C. Endogenous dBest1 in S2 cells was knocked down by RNAi that targeted the 5' UTR of dBest1 for 4 d. Cells were then transfected with dBest1-F81C and EGFP expression constructs and patch clamped in whole cell configuration with 10-s interval voltage ramps from -100 mV to $+100$ mV from a holding potential of 0 mV. Currents recorded from native S2 cells, dBest1 RNAi-treated S2 cells, and F81C overexpressed in dBest1 RNAi-treated S2 cells are labeled as native, RNAi, and F81C, respectively. (A) Current-voltage relationship of dBest1 currents in native and F81C-rescued cells recorded with $\Delta 0$ mosmol kg^{-1} isosmotic solutions. (B) Current-voltage relationship of dBest1 currents in native, F81C-rescued, and RNAi-only S2 cells stimulated with $\Delta 40$ mosmol kg^{-1} hyposmotic solutions. (C) Time course of activation of VRAC in S2 cells rescued with F81C. The currents shown were measured at -100 mV (open symbols) and $+100$ mV (solid symbols) under isosmotic (I300/E300, triangles; $n = 6$) and hyposmotic (I340/E300, circles; $n = 7$) conditions. (D) Mean current amplitudes at 100 mV at the onset of whole cell recording (initial current, open bars) and after the currents had reached a peak (final currents, filled

bars) and the corresponding cell volume alterations (hatched bars) with hyposmotic ($\Delta 40$ mosmol kg^{-1}) and isosmotic solutions. Changes in cell volume are expressed as percent change in cell volume from the initiation of whole cell recording to ~ 3 – 5 min after patch break (isosmotic; $n = 6$) or when the currents had approached a steady value (hyposmotic; $n = 7$). Data are represented in mean \pm SEM. *, significantly different at $P < 0.05$ and ** at $P < 0.01$ level.

F81C currents activated by hyposmotic solutions were reduced $\sim 60\%$ by MTSET $^+$, compared with an $\sim 20\%$ reduction for native dBest1 (Fig. 3, A and B). More importantly, MTSET $^+$ consistently produced an E_{rev} shift of

-19.9 ± 1.2 mV ($n = 12$) in F81C-rescued cells but not in native cells (Fig. 3 C). This negative shift in E_{rev} could be explained by a changed ionic selectivity of the channel. In these experiments, $[\text{Cl}^-]$ was the same on both sides

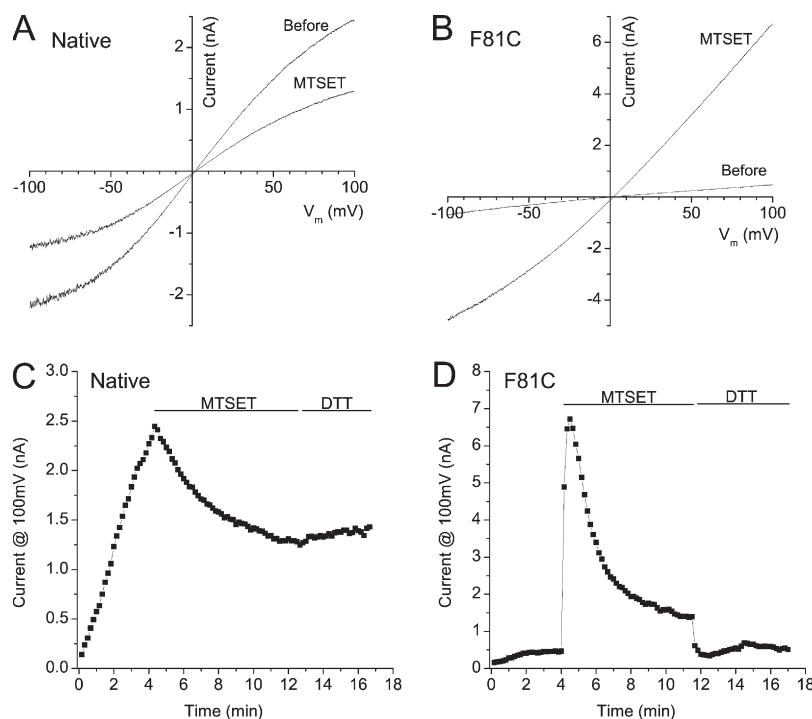


Figure 2. dBest1-F81C-rescued cells respond differently to MTSET $^+$ modification than native S2 cells. Whole cell VRAC currents were established in hyposmotic solutions (I340/E300, $\Delta 40$ mosmol kg^{-1}) and were recorded with voltage ramps from -100 to 100 mV. 1 mM MTSET $^+$ was applied to the bath solution (E300) after the volume-sensitive current was fully activated. The bath was then replaced with 5 mM DTT to test if the effect of MTSET $^+$ was reversible. (A and B) Current-voltage relationships in native (A) and dF81C-rescued (B) S2 cells before and after MTSET $^+$ modification. (C and D) Time course of the effect of MTSET $^+$ modification on native (C) and F81C-rescued (D) VRAC currents. These time course data were collected from the same cells shown in A and B.

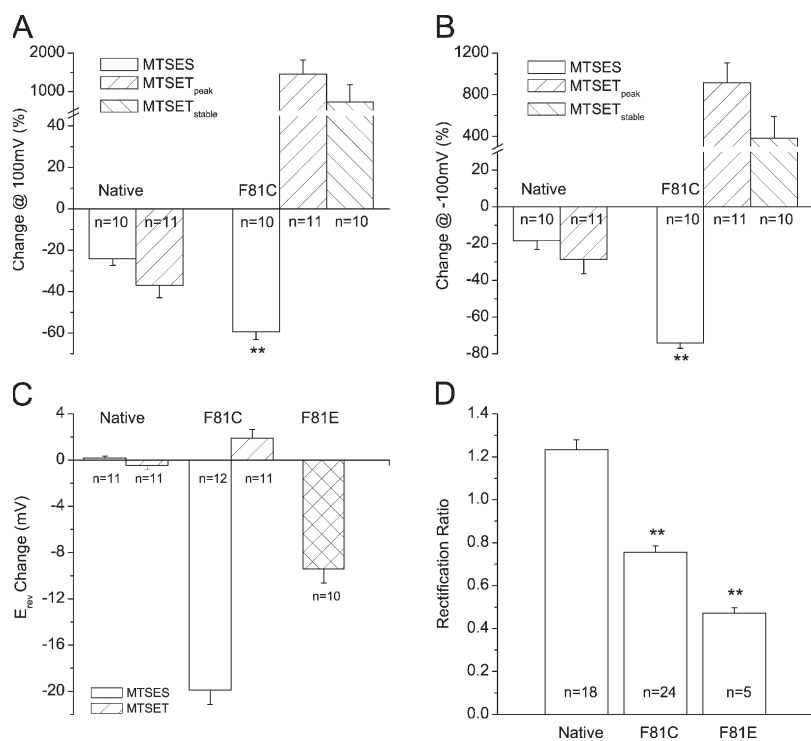


Figure 3. Summary of effects of mutations and sulfhydryl modification. The percent change was calculated using the following equation: $(I_{\text{MTS}} - I_{\text{before}}) / I_{\text{before}} \times 100\%$ for steady-state VRAC currents measured at 100 (A) and -100 mV (B), respectively. The effect of MTSES⁻ is shown in open bars, the peak stimulation after applying MTSET⁺ is shown as MTSET_{peak}, and the stabilized level in MTSET⁺ is shown as MTSET_{stable}. (C) Effect of MTS treatment on E_{rev} . The change in E_{rev} is the difference between E_{rev} before and after MTS treatment. The reversal potential of F81E currents (without MTS treatment) is shown with a cross-hatched bar. (D) Rectification ratio of native, F81C, and F81E VRAC currents. The rectification ratio was calculated as the absolute value of the VRAC current at $+100$ mV divided by the current at -100 mV for native, F81C, and F81E currents. Data are represented in mean \pm SEM. **, significantly different at $P < 0.01$ level.

of the membrane, so a pure Cl^- current would have an expected $E_{\text{rev}} = 0$ mV. The internal solution contained primarily Cs^+ and the external solution contained primarily Na^+ . Therefore, the MTSES⁻-induced negative shift in E_{rev} could be explained by an increased permeability to cations with $P_{\text{Cs}} > P_{\text{Na}}$. This hypothesis was qualitatively tested by replacing extracellular Na^+ with either Cs^+ or NMDG⁺ in the E300 solution while maintaining Cs^+ as the major intracellular cation (I340). The result from a typical F81C-rescued cell is shown in Fig. 4 C. Initially, F81C VRAC currents recorded with symmetrical Cl^- and Cs^+ inside and Na^+ outside had an E_{rev} of ~ 0 mV, as would be predicted if the F81C current were selectively carried by Cl^- . After MTSES⁻ was applied, E_{rev}

shifted to -25.1 mV. When extracellular Na^+ was replaced with Cs^+ , E_{rev} changed to 1.7 mV. Replacement of extracellular Cs^+ with the impermeant NMDG⁺ produced an E_{rev} shift to -38 mV. These observations suggested that the F81C current had become more permeable to Cs^+ and, less so, to Na^+ after MTSES⁻ modification.

To quantify relative cation⁺/ Cl^- permeability, we performed dilution potential experiments (Franciolini and Nonner, 1987) for native dBest1, F81C, and F81E currents. For these experiments, we chose to activate the current by high intracellular Ca^{2+} because the dBest1 current activated by cell swelling often ran down after the current was fully activated, making several E_{rev} determinations in the same cell problematic. In contrast, the

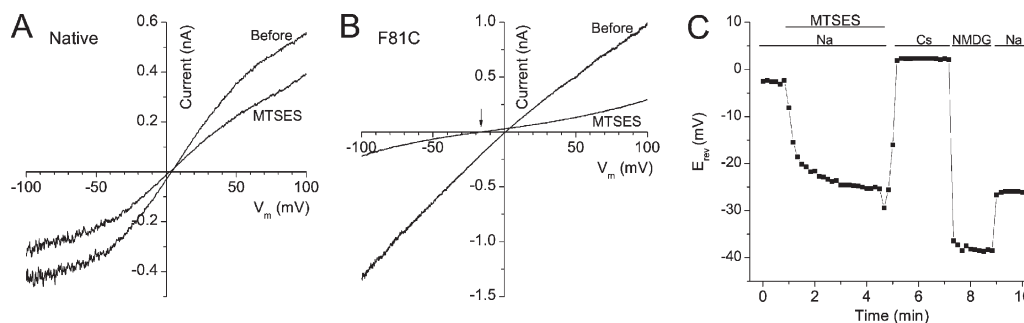


Figure 4. MTSES⁻ increases the cation permeability of F81C currents. Current-voltage relationships from a typical native S2 cell (A) and a S2 cell rescued with F81C (B) before and after MTSES⁻ modification. Currents were activated with $\Delta 40$ mosmol kg^{-1} hyposmotic solutions. The arrow in B points out the reversal potential of F81C current after MTSES⁻ treatment. (C) Changes in E_{rev} of F81C currents under different ionic conditions. The record begins after the dBest1 current had stabilized under hyposmotic solutions (I340/E300, $\Delta 40$ mosmol kg^{-1}). MTSES⁻ was then applied in the bath. Extracellular solution containing symmetrical Cl^- and Na^+ as the major cation (E300) was then replaced by solutions with Cs^+ or NMDG⁺ as the major cations as indicated. The osmolality of all the extracellular solutions was 300 mosmol kg^{-1} .

Ca^{2+} -activated dBest1 current does not run down significantly for up to 10 min. The nature of this rundown and why it is only seen when dBest1 current is activated by hyposmotic cell swelling but not by Ca^{2+} are not clear. Nevertheless, we chose to activate dBest1 current by intracellular application of Ca^{2+} to obtain data to avoid the possible interference of the rundown. Cells were treated with MTSES⁻, and E_{rev} was measured with 150 mM CsCl inside and various concentrations of CsCl outside. I-V curves from typical cells recorded with 10, 50, and 150 mM external CsCl are superimposed in Fig. 5 (A–C). For native dBest1 currents (Fig. 5 A), E_{rev} moved toward positive values as external [CsCl] was decreased, as would be predicted if dBest1 is selectively permeable to Cl^- . In addition, the conductance in the outward direction at +100 mV increased significantly with increasing external [CsCl], consistent with Cl^- carrying the majority of the outward current. In contrast, the E_{rev} of F81C shifted toward negative potentials with decreasing external [CsCl] (Fig. 5 B). This negative shift in E_{rev} showed that F81C had become more selective to Cs^+ than to Cl^- after MTSES⁻ modification. The augmented inward rectification with increasing external [CsCl] was also consistent with a higher Cs^+ conductance relative to Cl^- after MTSES⁻ treatment.

Relative Cs^+/Cl^- permeability was calculated by fitting the plots of E_{rev} versus [CsCl]_o to the GHK equation. As shown in Fig. 5 D, the mean E_{rev} in native S2 cells shifted on average $+33.3 \pm 3.2$ mV with a 15-fold decrease in [CsCl]_o (●). The data were well-fitted by

the GHK equation, assuming that Cl^- was fourfold more permeable than Cs^+ ($P_{\text{Cs}}/P_{\text{Cl}} = 0.25$). dBest1-F81C, on the other hand, showed a shift in the opposite direction of -22.8 ± 2.3 mV with a 15-fold decrease in [CsCl]_o (Fig. 5 D, ▲), which was fitted to $P_{\text{Cs}}/P_{\text{Cl}} = 2.38$. The $P_{\text{Cs}}/P_{\text{Cl}}$ ratio in rescued cells overexpressing wild-type dBest1 was the same as the native S2 current regardless of MTSES⁻ treatment ($P_{\text{Cs}}/P_{\text{Cl}} = 0.24$; not depicted), indicating that the switch in ionic selectivity in F81C currents was not due to an up-regulation of an endogenous cation channel.

The ionic selectivity of dBest1 was explored further by replacing the F81 residue with the negatively charged amino acid, glutamic acid (E). We discovered that the F81E current reversed at -9.4 ± 1.2 mV under conditions of symmetrical Cl^- and Cs^+ inside and Na^+ outside (Fig. 3 C). This is significantly different from the native current (0.2 ± 0.2 mV). $P_{\text{Cs}}/P_{\text{Cl}}$ for F81E was calculated to be 1.33 from dilution potential experiments (Fig. 5, C and D). Furthermore, the F81E current inwardly rectified (Fig. 3 D). The fact that F81E qualitatively recapitulated most of the properties of MTSES⁻-modified F81C currents provided additional support that residue F81 is in vicinity to the ion selectivity filter of the dBest1 Cl^- channel.

The dilution potential experiment was repeated with NaCl replacing CsCl. The native dBest1 channel was highly selective to Cl^- relative to Na^+ and was fitted with a $P_{\text{Na}}/P_{\text{Cl}}$ ratio of 0.03 (Fig. 5 D). MTSES⁻-modified F81C, on the other hand, was almost equally permeable to Cl^- and Na^+ ($P_{\text{Na}}/P_{\text{Cl}} = 0.83$) (Fig. 5 D).

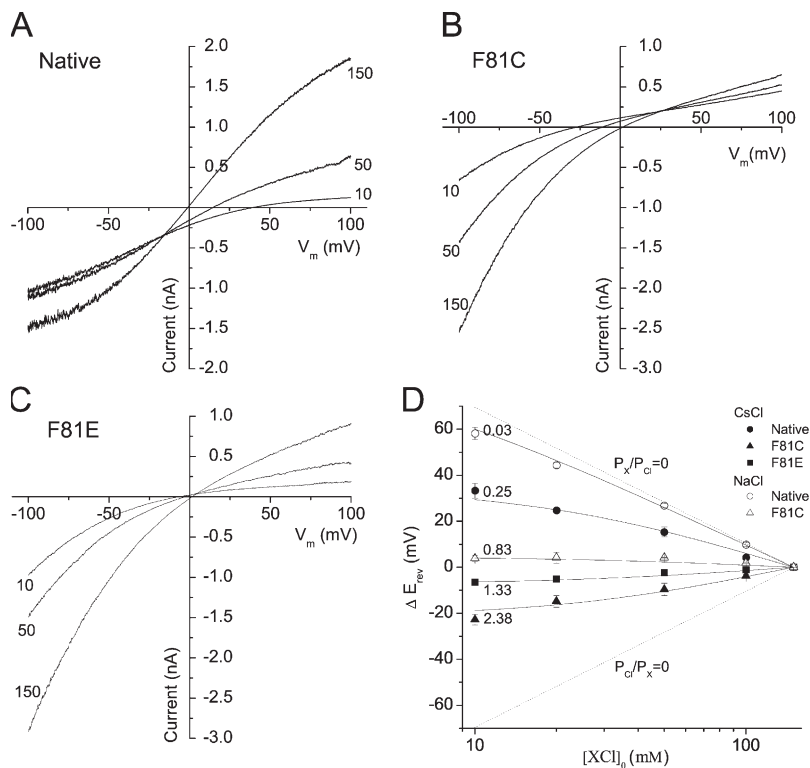


Figure 5. Quantification of relative cation/chloride permeability. Current–voltage relationships of MTSES⁻-modified native (A) and F81C (B) currents and unmodified F81E currents (C) in response to different external [CsCl]. Whole cell currents were activated under isosmotic condition ($304 \text{ mosmol kg}^{-1}$) with high Ca^{2+} in the pipet and symmetrical CsCl in the bath and pipet (150 mM). The extracellular solution was replaced by solutions containing different [CsCl] as indicated. (D) Changes in E_{rev} (ΔE_{rev}) as a function of extracellular salt concentration. ΔE_{rev} is E_{rev} at the indicated salt concentration minus the E_{rev} with 150 mM extracellular salt. Salt is either CsCl or NaCl as indicated. Each data point represents the mean $E_{\text{rev}} \pm \text{SEM}$ of two to nine cells. Dashed lines were calculated from the GHK equation ($\Delta E_{\text{rev}} = 25.7 \cdot \ln \left(\frac{([X^+]_o + [\text{Cl}^-]_i) \cdot P_{\text{Cl}}/P_X}{([X^+]_i + [\text{Cl}^-]_o) \cdot P_{\text{Cl}}/P_X} \right)$), assuming that the channel is exclusively permeable to Cl^- ($P_X/P_{\text{Cl}} = 0$) or to the cation X^+ ($P_{\text{Cl}}/P_X = 0$). Filled symbols: CsCl solutions; ●, MTSES⁻-treated native dBest1 ($n = 2-7$); ▲, MTSES⁻-modified F81C ($n = 4-9$); ■, F81E ($n = 2-5$). Open symbols: NaCl solutions; ○, MTSES⁻-treated native dBest1 ($n = 3-5$); △, F81C ($n = 3-8$).

The role of dBest1 in forming the pore of the channel was further tested in HEK cells transfected with either wild-type dBest1 or F81C. The dilution potential experiment was repeated in transfected HEK cells either with or without MTSES[−] treatment (Fig. 6). Wild-type dBest1 in the presence or absence of MTSES[−] and F81C dBest1 in the absence of MTSES[−] exhibited similar $P_{\text{Cs}}/P_{\text{Cl}}$ ratios (~ 0.1). In contrast, the MTSES[−]-modified F81C channel exhibited a significantly elevated cation permeability ($P_{\text{Cs}}/P_{\text{Cl}} = 0.50$). Despite the observation that the change in ionic selectivity is smaller in HEK cells than in S2 cells, MTSES[−] modification still caused a significant shift of ionic selectivity. We do not understand why there is a quantitative difference between HEK cells and S2 cells. It appears that there may be different factors or subunits in these two cell types that contribute to channel selectivity.

VRAC in Macrophages from Bestrophin Knockout Mice

To test whether bestrophins are responsible for VRAC in mammals, we measured VRAC in peritoneal macrophages from wild-type mice and mice that had both mBest1 and mBest2 disrupted (Fig. 7). VRAC in these cells was activated by changing extracellular osmolality from either 306 mosmol kg^{−1} (isosmotic) or 326 mosmol kg^{−1} ($\Delta 20$ hyperosmotic) to 266 mosmol kg^{−1} ($\Delta 40$ hyposmotic) or 234 mosmol kg^{−1} ($\Delta 70$ hyposmotic). The amplitude of VRAC in the wild-type and knockout animals was statistically the same. These results show that mBest1 and mBest2 are not required for VRAC in peritoneal macrophages and suggest that other kinds of channels are responsible for VRAC in mammalian cells.

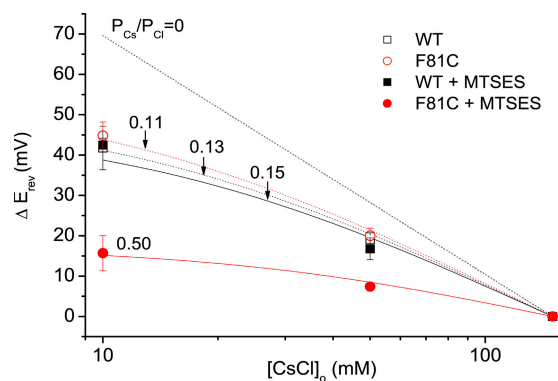


Figure 6. Quantification of relative Cs^+/Cl^- permeability in HEK cells transfected with dBest1. Whole cell current was measured in wild-type dBest1 or dBest1-F81C-overexpressed HEK cells. Changes in E_{rev} (ΔE_{rev}) as a function of extracellular CsCl concentration were plotted for cells with and without MTSES[−] treatment. Each data point represents the mean $E_{\text{rev}} \pm \text{SEM}$ of two to seven cells. Gray dashed line was calculated from the GHK equation assuming that the channel is exclusively permeable to Cl^- ($P_{\text{Cs}}/P_{\text{Cl}} = 0$). Filled symbols: MTSES[−]-treated; \bullet , F81C ($n = 2-7$); \blacksquare , wild-type dBest1 ($n = 3-4$). Open symbols: without MTSES[−] treatment; \circ , wild-type dBest1 ($n = 5$); \square , F81C ($n = 3$).

DISCUSSION

We have previously shown that the dBest1 current plays an essential role in RVD in S2 cells because RNAi knockdown of dBest1 largely eliminates RVD (Chien and Hartzell, 2007). Our previous data did not clearly establish that dBest1 formed the channel, however, because RNAi knockdown of an essential regulator or β -subunit of the channel would have the same effect as knocking down the channel itself. To establish that dBest1 is the channel itself, it was necessary to rescue the current with a channel that had a biophysical signature that was clearly different than the wild-type channel. Our results here provide solid support that dBest1 is indeed the VRAC in *Drosophila* S2 cells because we were able to rescue the volume-regulated current by overexpressing a mutant dBest1 with altered biophysical properties. The rescued current is clearly sensitive to cell volume; in hyposmotic solution, the current increases with time in parallel with cell swelling. The F81C mutant current has several hallmark features. (1) F81C exhibits altered rectification. The rectification ratio was ~ 0.8 for F81C compared with ~ 1.2 for native currents. (2) MTSES[−] modification of the F81C channel altered the ionic selectivity of the channel so that the channel became more permeable to cations than to Cl^- . (3) F81C current amplitude was stimulated by MTSET⁺, whereas the wild-type current was decreased slightly. These three distinguishing features show clearly that the rescued current is mediated by dBest1-F81C. It is difficult to imagine how dBest1 could produce these changes if it were merely a regulatory subunit of the channel. These results with F81C are strengthened by the observation that the F81E mutant also has an increased permeability to cations compared with the wild-type current.

The volume sensitivity of the rescued current (both wild-type and F81C) is slightly different than the native VRAC current. Typically, the native VRAC current immediately after breaking the patch to initiate whole cell recording is ~ 0.1 nA or less at +100 mV, whereas with the F81C mutant the current is ~ 0.4 nA. Because the osmotic pressure difference develops only after the patch is broken, the observation that the initial F81C current is larger than native current suggests that the F81C current is partially activated before patch break. Furthermore, the rescued currents seem to activate more quickly than the native current. We believe that these differences are an artifact of overexpression; the channel may be partially uncoupled from its regulatory mechanisms and exhibit a different “set-point.” This is supported by the observation that the apparent uncoupling is related to the level of overexpression. With high levels of overexpression of wild-type dBest1, currents are observed even under isosmotic conditions.

Despite this rather compelling evidence that dBest1 is the VRAC in S2 cells, it seems unlikely that bestrophins constitute the VRAC family in mammals because VRAC

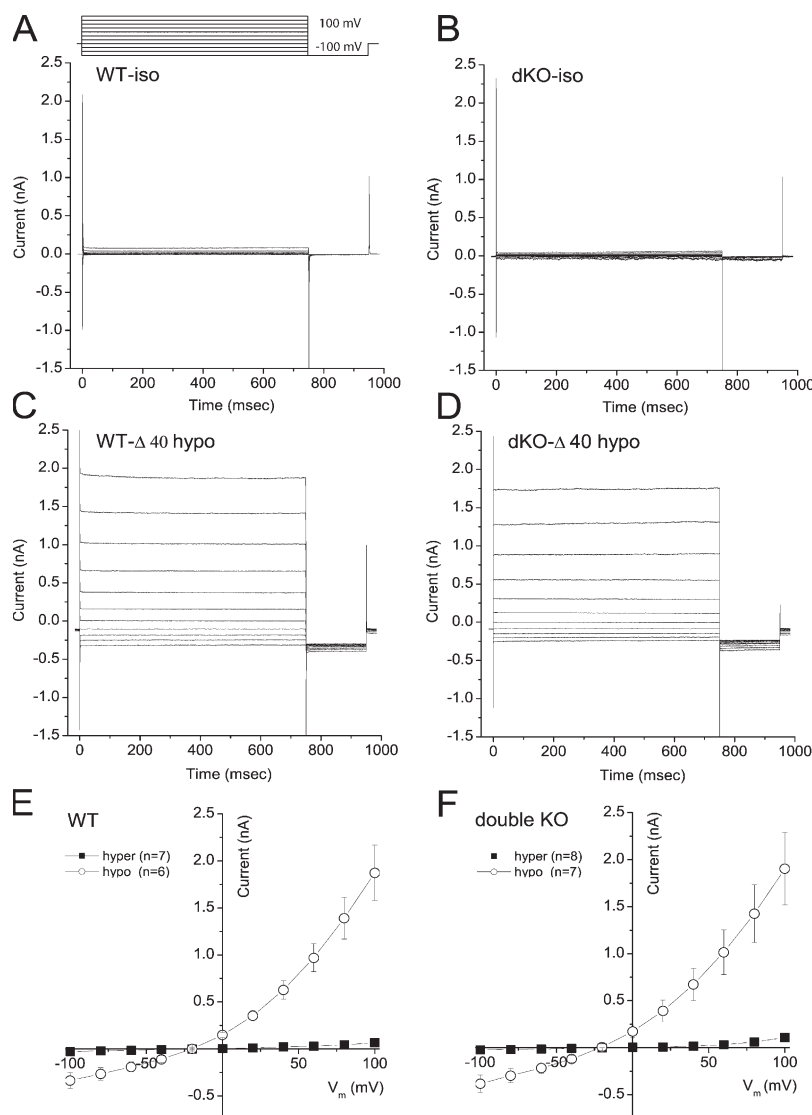


Figure 7. VRAC in peritoneal macrophages from wild-type and mBest1^{-/-}mBest2^{-/-} mice. (A, C, and E) Wild-type mice. (B, D, and F) mBest1^{-/-}mBest2^{-/-} mice. The intracellular solution of all recordings was held constant at 306 mosmol kg⁻¹, whereas the osmolality of the extracellular solution was altered to achieve different osmotic pressures. (A and B) Current traces under isosmotic conditions. (C and D) Current traces in $\Delta 40$ mosmol kg⁻¹ hypotonic conditions (266 mosmol kg⁻¹ extracellular). (E and F) Average current-voltage relationships under $\Delta 70$ mosmol kg⁻¹ hypotonic (open symbols; 234 mosmol kg⁻¹ extracellular) and $\Delta 20$ mosmol kg⁻¹ hyperosmotic (filled symbols; 326 mosmol kg⁻¹ extracellular) conditions.

is unaffected in macrophages from mice with both mBest1 and mBest2 knocked out. A less extensive examination of VRAC in microglia also revealed no obvious difference between wild-type and knockout (not depicted). Mice have three functional bestrophin genes, but it seems unlikely that VRAC in microglia and macrophages can be explained by the one bestrophin we have not knocked out. hBest1 and mBest2 have both been shown to exhibit sensitivity to cell volume (Fischmeister and Hartzell, 2005), but if bestrophins are VRACs, one would expect that they would be expressed ubiquitously. But, the data on bestrophin expression suggests that they have rather restricted tissue expression. Publicly available microarray and electronic Northern data (<http://www.genecards.org>) are limited, and published reports of bestrophin expression by RT-PCR, Northern, and immunoblotting or immunostaining are not always in agreement (Hartzell et al., 2008). At this point in time, the most conservative interpretation is that bestrophins may be one of many different kinds of channels that play a role in cell volume

regulation (Nilius et al., 1996; Strange et al., 1996; Lang et al., 1998) or, possibly, that Cl⁻ fluxes associated with cell volume changes are not mediated by specific ion channels, but rather by Cl⁻-interacting proteins that have other primary functions.

The ability to change the anionic selectivity of dBest1 from anionic to cationic by MTSES⁻ modification of a point mutant is surprising and may shed light on the mechanisms involved in ion permeation through bestrophin channels. In S2 cells, the MTSES⁻-modified F81C current exhibits a P_{Na}/P_{Cl} ratio of 0.83 and a P_{Cs}/P_{Cl} ratio of 2.38. This suggests that the permeability sequence is $P_{Cs} > P_{Cl} > P_{Na}$. This is supported by the observation that E_{rev} shifted to more negative potentials when extracellular Cs⁺ is replaced with the impermeant NMDG⁺ than with Na⁺. Other examples of ion channels where the charge selectivity has been reversed include the nicotinic ACh receptor (Galzi et al., 1992), the GABA_A receptor (Wang et al., 1999), and the glycine receptor (Keramidas et al., 2000, 2002). Keramidas et al. (2000, 2002)

have converted the glycine receptor from Cl^- selective to cation selective by introducing a negative charge in the M2 pore-forming segment by changing A215 to glutamate. The cationic permeability is enhanced by deleting a proline at position 250, which alters the structure and diameter of the pore (Keramidas et al., 2002). The double mutant of the glycine receptor exhibits a permeability sequence of $P_{\text{Cs}} > P_{\text{Na}} > P_{\text{Cl}}$ (1.7: 1.0: 0.13). The changes that we observe with the F81C mutant of dBest1 are similar to the single A215E glycine receptor mutant, but less dramatic than those in the glycine receptor double mutant. Perhaps mutation of additional amino acids in dBest1 may produce larger effects. It is significant that changing F81 to glutamate has a smaller effect than modifying the F81C mutant with MTSES $^-$. This may be explained by the fact that MTSES $^-$ is a rather large molecule (1.2 nm \times 0.6 nm; Kaplan et al., 2000) compared with the dimensions of glutamate or cysteine (side chain length of <0.5 nm). Thus, the negative charge provided by MTSES $^-$ is likely to be positioned differently than the negative charge provided by glutamate. The reversal in charge selectivity produced by MTSES $^-$, therefore, may involve other regions of dBest1 in addition to transmembrane domain 2, where F81 is located. It is also possible that the incorporation of the MTSES $^-$ moiety disrupts the structure of the pore and changes its diameter or other properties. However, the effect of MTSES $^-$ on ionic selectivity of F81C expressed in HEK cells was less than when F81C was expressed in S2 cells. These data suggested that the bestrophin channel might involve other proteins to form the pore.

The second transmembrane domain of hBest1 is a hot-spot for disease-causing mutations (Hartzell et al., 2008). One of the disease-causing mutations is F80L. Although we have not tested this mutation in hBest1, the F81L mutation in dBest1 is nonfunctional. This emphasizes the importance of the second transmembrane domain in bestrophin function.

We would like to especially thank Dr. Zhiqiang (Sean) Qu for his kindly assistance in providing some data on the effect of MTSES on native dBest1 VRAC currents and for helpful discussion, Yuanyuan Cui for her wonderful technical assistance, and Dr. David Clapham for constantly reminding us that we are probably wrong. Best1 and Best2 knockout mice were kindly provided by Dr. Kosta Petrukhin (Merck & Co.) and Dr. Alan Marmorstein (University of Arizona).

This research is supported by National Institutes of Health grants GM60448 and EY014852.

Edward N. Pugh served as editor.

Submitted: 16 June 2008

Accepted: 29 September 2008

REFERENCES

Bakall, B., P. McLaughlin, J.B. Stanton, Y. Zhang, H.C. Hartzell, Y.L. Marmorstein, and A.D. Marmorstein. 2008. Bestrophin-2 is involved in the generation of intraocular pressure. *Invest. Ophthalmol. Vis. Sci.* 49:1563–1570.

Barro Soria, R., M. Spitzner, R. Schreiber, and K. Kunzelmann. 2006. Bestrophin 1 enables Ca^{2+} activated Cl^- conductance in epithelia. *J. Biol. Chem.* 10.1074/jbc.M605716200.

Burgess, R., I.D. Millar, B.P. Leroy, J.E. Urquhart, I.M. Fearon, B.E. De, P.D. Brown, A.G. Robson, G.A. Wright, P. Kestelyn, et al. 2008. Biallelic mutation of BEST1 causes a distinct retinopathy in humans. *Am. J. Hum. Genet.* 82:19–31.

Chien, L.T., and H.C. Hartzell. 2007. *Drosophila* bestrophin-1 chloride current is dually regulated by calcium and cell volume. *J. Gen. Physiol.* 130:513–534.

Chien, L.T., Z.R. Zhang, and H.C. Hartzell. 2006. Single Cl^- channels activated by Ca^{2+} in *Drosophila* S2 cells are mediated by bestrophins. *J. Gen. Physiol.* 128:247–259.

Fischmeister, R., and C. Hartzell. 2005. Volume sensitivity of the bestrophin family of chloride channels. *J. Physiol.* 552:477–491.

Franciolini, F., and W. Nonner. 1987. Anion and cation permeability of a chloride channel in rat hippocampal neurons. *J. Gen. Physiol.* 90:453–478.

Galzi, J.L., A. Devillers-Thiery, N. Hussy, S. Bertrand, J.P. Changeux, and D. Bertrand. 1992. Mutations in the channel domain of a neuronal nicotinic receptor convert ion selectivity from cationic to anionic. *Nature.* 359:500–505.

Guziewicz, K.E., B. Zangerl, S.J. Lindauer, R.F. Mullins, L.S. Sandmeyer, B.H. Grahn, E.M. Stone, G.M. Acland, and G.D. Aguirre. 2007. Bestrophin gene mutations cause canine multifocal retinopathy: a novel animal model for best disease. *Invest. Ophthalmol. Vis. Sci.* 48:1959–1967.

Hartzell, H.C., Z. Qu, K. Yu, Q. Xiao, and L.T. Chien. 2008. Molecular physiology of bestrophins: multifunctional membrane proteins linked to best disease and other retinopathies. *Physiol. Rev.* 88:639–672.

Hille, B. 2001. *Ion Channels of Excitable Membranes*. 3rd edition. Sinauer Associates Inc. Sunderland, MA. 814 pp.

Kaplan, R.S., J.A. Mayor, D. Brauer, R. Kotaria, D.E. Walters, and A.M. Dean. 2000. The yeast mitochondrial citrate transport protein. Probing the secondary structure of transmembrane domain IV and identification of residues that likely comprise a portion of the citrate translocation pathway. *J. Biol. Chem.* 275:12009–12016.

Keramidas, A., A.J. Moorhouse, C.R. French, P.R. Schofield, and P.H. Barry. 2000. M2 pore mutations convert the glycine receptor channel from being anion- to cation-selective. *Biophys. J.* 79:247–259.

Keramidas, A., A.J. Moorhouse, K.D. Pierce, P.R. Schofield, and P.H. Barry. 2002. Cation-selective mutations in the M2 domain of the inhibitory glycine receptor channel reveal determinants of ion-charge selectivity. *J. Gen. Physiol.* 119:393–410.

Lang, F., G.L. Busch, M. Ritter, H. Volkl, S. Waldegger, E. Gulbins, and D. Haussinger. 1998. Functional significance of cell volume regulatory mechanisms. *Physiol. Rev.* 78:247–306.

Marmorstein, A.D., and T.R. Kinnick. 2007. Focus on molecules: bestrophin (Best-1). *Exp. Eye Res.* 85:423–424.

Marmorstein, A.D., R. Rosenthal, J.B. Stanton, B. Bakall, C. Wadelius, L.Y. Marmorstein, A.F.X. Goldberg, N. Peachey, and O. Strauss. 2004a. Bestrophin is not a chloride channel. *ARVO Meeting Abstracts* 45:1759.

Marmorstein, A.D., J.B. Stanton, J. Yocom, B. Bakall, M.T. Schiavone, C. Wadelius, L.Y. Marmorstein, and N.S. Peachey. 2004b. A model of best vitelliform macular dystrophy in rats. *Invest. Ophthalmol. Vis. Sci.* 45:3733–3739.

Marmorstein, L.Y., J. Wu, P. McLaughlin, J. Yocom, M.O. Karl, R. Neusser, S. Wimmers, J.B. Stanton, R.G. Gregg, O. Strauss, et al. 2006. The light peak of the electroretinogram is dependent on voltage-gated calcium channels and antagonized by bestrophin (Best-1). *J. Gen. Physiol.* 127:577–589.

Marquardt, A., H. Stohr, L.A. Passmore, F. Kramer, A. Rivera, and B.H. Weber. 1998. Mutations in a novel gene, VMD2, encoding

- a protein of unknown properties cause juvenile-onset vitelliform macular dystrophy (Best's disease). *Hum. Mol. Genet.* 7:1517–1525.
- Nilius, B., J. Eggermont, T. Voets, and G. Droogmans. 1996. Volume-activated Cl⁻ channels. *Gen. Pharmacol.* 27:1131–1140.
- Petrukhin, K., M.J. Koisti, B. Bakall, W. Li, G. Xie, T. Marknell, O. Sandgren, K. Forsman, G. Holmgren, S. Andreasson, et al. 1998. Identification of the gene responsible for Best macular dystrophy. *Nat. Genet.* 19:241–247.
- Qu, Z., and H.C. Hartzell. 2004. Determinants of anion permeation in the second transmembrane domain of the mouse bestrophin-2 chloride channel. *J. Gen. Physiol.* 124:371–382.
- Qu, Z., R.W. Wei, W. Mann, and H.C. Hartzell. 2003. Two bestrophins cloned from *Xenopus laevis* oocytes express Ca-activated Cl currents. *J. Biol. Chem.* 278:49563–49572.
- Qu, Z., R. Fischmeister, and H.C. Hartzell. 2004. Mouse bestrophin-2 is a bona fide Cl⁻ channel: identification of a residue important in anion binding and conduction. *J. Gen. Physiol.* 123:327–340.
- Qu, Z., Y. Cui, and C. Hartzell. 2006a. A short motif in the C-terminus of mouse bestrophin 4 inhibits its activation as a Cl channel. *FEBS Lett.* 580:2141–2146.
- Qu, Z., L.T. Chien, Y. Cui, and H.C. Hartzell. 2006b. The anion-selective pore of the bestrophins, a family of chloride channels associated with retinal degeneration. *J. Neurosci.* 26:5411–5419.
- Rosenthal, R., B. Bakall, T. Kinnick, N. Peachey, S. Wimmers, C. Wadelius, A. Marmorstein, and O. Strauss. 2005. Expression of bestrophin-1, the product of the VMD2 gene, modulates voltage-dependent Ca²⁺ channels in retinal pigment epithelial cells. *FASEB J.* 20:178–180.
- Seddon, J.M., M.A. Afshari, S. Sharma, P.S. Bernstein, S. Chong, A. Hutchinson, K. Petrukhin, and R. Allikmets. 2001. Assessment of mutations in the best macular dystrophy (VMD2) gene in patients with adult-onset foveomacular vitelliform dystrophy, age-related maculopathy, and bull's-eye maculopathy. *Ophthalmology.* 108:2060–2067.
- Strange, K., F. Emma, and P.S. Jackson. 1996. Cellular and molecular physiology of volume-sensitive anion channels. *Am. J. Physiol.* 270:C711–C730.
- Sun, H., T. Tsunenari, K.-W. Yau, and J. Nathans. 2002. The vitelliform macular dystrophy protein defines a new family of chloride channels. *Proc. Natl. Acad. Sci. USA.* 99:4008–4013.
- Tsunenari, T., H. Sun, J. Williams, H. Cahill, P. Smallwood, K.-W. Yau, and J. Nathans. 2003. Structure-function analysis of the bestrophin family of anion channels. *J. Biol. Chem.* 278:41114–41125.
- Tsunenari, T., J. Nathans, and K.W. Yau. 2006. Ca²⁺-activated Cl⁻ current from human bestrophin-4 in excised membrane patches. *J. Gen. Physiol.* 127:749–754.
- Wang, C.T., H.G. Zhang, T.A. Rocheleau, R.H. French-Constant, and M.B. Jackson. 1999. Cation permeability and cation-anion interactions in a mutant GABA-gated chloride channel from *Drosophila*. *Biophys. J.* 77:691–700.
- Yardley, J., B.P. Leroy, N. Hart-Holden, B.A. Lafaut, B. Loeys, L.M. Messiaen, R. Perveen, M.A. Reddy, S.S. Bhattacharya, E. Traboulsi, et al. 2004. Mutations of VMD2 splicing regulators cause nanophthalmos and autosomal dominant vitreoretinopathy (ADVIRC). *Invest. Ophthalmol. Vis. Sci.* 45:3683–3689.
- Yu, K., Q. Xiao, G. Cui, A. Lee, and H.C. Hartzell. 2008. The best disease-linked Cl⁻ channel hBest1 regulates CaV1 (L-type) Ca²⁺ channels via src-homology-binding domains. *J. Neurosci.* 28:5660–5670.